J. Phase Equilib. Diffus.
https://doi.org/10.1007/s11669-023-01033-3

A Mathematical Computer Model for Estimating Phase Weight/Atomic Fractions for Iron Slags' System (SiO_2-Al_20_3-CaO-MgO) at Subsolidus Temperatures

Tanju Yelkenci[1] · **Z. Engin Erkmen**[2]

Submitted: 12 December 2022 / in revised form: 14 February 2023 / Accepted: 1 March 2023

Abstract In this study, the 3 dimensional description of the quaternary subsolidus slag system aluminasilicacalcia-magnesia is evaluated using Mathematica programming based on previous experimental research data. The lever rule in the tetrahedra is then applied for a given arbitrary liquid composition A% + %B + %C + %D = 100 in order to calculate the solid phases present (neglecting solid solutions) with their relative proportions after the solidification is completed. A novel transformation and algorithm are then developed using simple geometry and MathLab programming which can also be used for other subsolidus systems in case appropriate data are provided.

Keywords iron steel slag · mathematical model · quaternary system · subsolidus equilibrium

1 Introduction

Ternary/Quaternary phase equilibrium diagrams are the milestones for determining phases and their corresponding wt. (or at.)% and their concentrations under equilibrium conditions in multicomponents, multiphase systems at given pressures and temperatures. The system Al_2O_3-MgO-SiO_2-CaO is one of the most studied in the oxide field due to its applications in blast furnace slags, bioceramics, cement production, refractories, glasses and technical ceramics. The phase compatibility model of the system is derived from the literature data and built in 3 dimensions using solid wood and cords and using Mathematica programming based on the geometrical consideration. Fifty one equilibrium quaternary phase assemblages have been established, which define the entire subsolidus phase space based on data given in Ref 1. There are so far very few studies on iron and steel slags that include quaternary descriptions.[2–4] Vasquez et al.[5,6] studied the crystallization volume of alumina in the Al_2O_3-MgO-SiO_2-CaO system and the invariants points were determined in compatibility tetrahedrons Al_2O_3 + $MgAl_2O_4$ + $Al_6Si_2O_{13}$ + $CaAl_2Si_2O_8$(anorthite) and Al_2O_3 + $MgAl_2O_4$ + $CaAl_2Si_2O_8$ + $CaAl_2O_{19}$ which are also presented in our descriptive model. A general summary of quaternary systems can be found in Hummel's[7] and Cox et al.'s textbooks[8] in Chapter 8. Lutsyk et al. worked on T-x-y-z diagrams invariant point determination by the geometrical computation and mainly based on intersecting planes for findings invariant points to find out the compositions and claimed to predict the view of horizontal or vertical sections.[9] The three dimensional descriptive model of Al_2O_3-MgO-SiO_2-CaO system in the present work excluding solid solutions is based essentially on previous research.[10–12] Preliminary studies for determining the phase distribution were started in the second half of the previous century by Devries and Osborn[13] and kinetic studies of the slag crystallization were performed by Erkmen et al.[14] and Lai et al.[15] and specific compositions under specific basicity and CaO/SiO_2 ratio were studied by Kou et al.[16] and Wang et al.[17], respectively.

A join connecting the compositions of the primary crystals of two primary fields in two dimensional ternary

✉ Tanju Yelkenci
tanju.yelkenci@tau.edu.tr

Z. Engin Erkmen
eerkmen@marmara.edu.tr

[1] Turkish-German University, Faculty of Engineering, 34820 Istanbul, Turkey

[2] Marmara University, Faculty of Engineering, 34854 Istanbul, Turkey

Published online: 31 March 2023

system or two volumes in three dimensional quaternary system having a common boundary line or surface respectively is called an Alkemade line. Thus it is essential that for an Alkemade line to exist, common phase boundaries/surfaces should exist between components.

Besides the existing thermodynamical software developed for estimating phase states and their corresponding weight/atomic fractions for the given input pressures, temperatures and concentrations, the developed model is based on pure mathematical and geometrical principles provided that the compositional data of binary and ternary compounds in any existing quaternary systems are supplied as the input. Any arbitrary quaternary composition chosen will essentially be located in one of the compatibility tetrahedra for which at the end of slow cooling, below solidus, the equilibrium phases will be those at the apices of the tetrahedron; their weight or molecular percentages will then be calculated applying the lever rule.

2 Method

The Mathematica programming is used to draw the Figures of the tetrahedron while the MathLab. programming is used for developing the algorithm. First, the coordinates of the 4 apices of a tetrahedron given in Fig. 1 are calculated in the Cartesian coordinate system.

$Al_2O_3 = \{-50, 0, 0\}$

$MgO = \{0, 86.6, 0\}$

$SiO_2 = \{50, 0, 0\}$

$CaO = \{0, 28.87, 81.65\}$

Next, the mathematical direct (and reverse transformations) of the existing compositions from the quaternary system (A%, B%, C%, D%) to the cartesian coordinate system (x, y, z) are derived. Using the direct transformations the xyz coordinates of the existing compounds in quaternary system are calculated and given as:

$CS = \{25.86, 13.93, 39.4\}, C3S2 = \{20.83, 16.84, 47.63\},\ C2S = \{17.45, 18.79, 53.16\},\ C3S = \{13.15, 21.27, 60.16\},\ C3A = \{-18.88, 17.96, 50.80\},\ C12A7 = \{-25.75, 13.99, 39.58\},\ CA = \{-32.27, 10.23, 28.93\},\ CA2 = \{-39.23, 6.06, 17.14\},\ CA6 = \{-45.80, 2.42, 6.84\},\ A3S2 = \{-21.83,\ 0,\ 0\},\ CAS2 = \{3.23, 5.77, 16.33\},\ C2AS = \{-7.5, 11.83, 33.48\},\ M2A2S5 = \{8.25, 11.90,\ 0\},\ M2S = \{21.35, 49.62,\ 0\},\ MS = \{29.9, 34.72,\ 0\}$

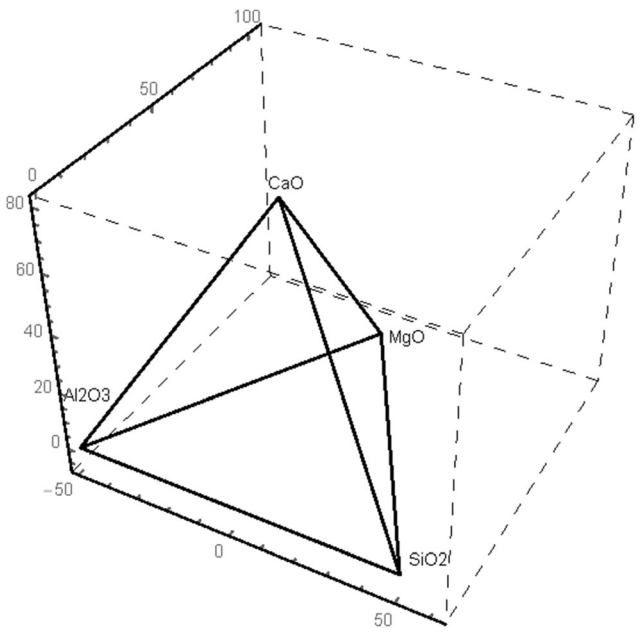

Fig. 1 Three dimensional model of Al_2O_3-MgO-SiO_2-CaO quaternary system

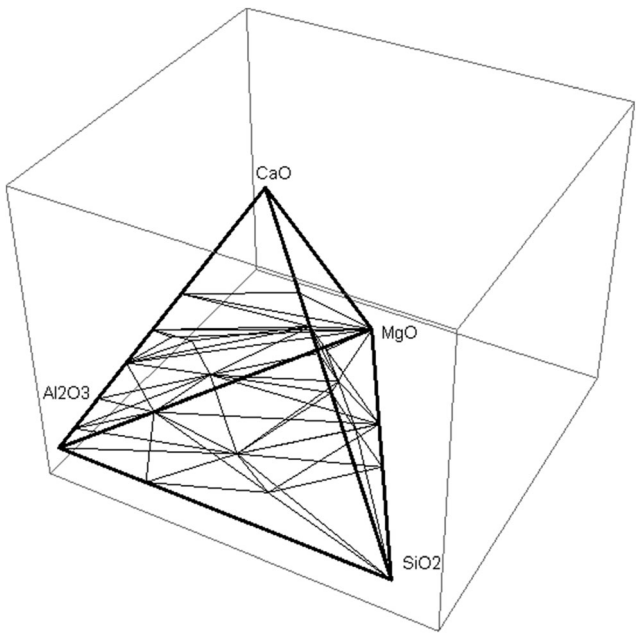

Fig. 2 3 Dimensional modelling of quaternary equilibrium system Al_2O_3-MgO-SiO_2-CaO system below solidus temperature

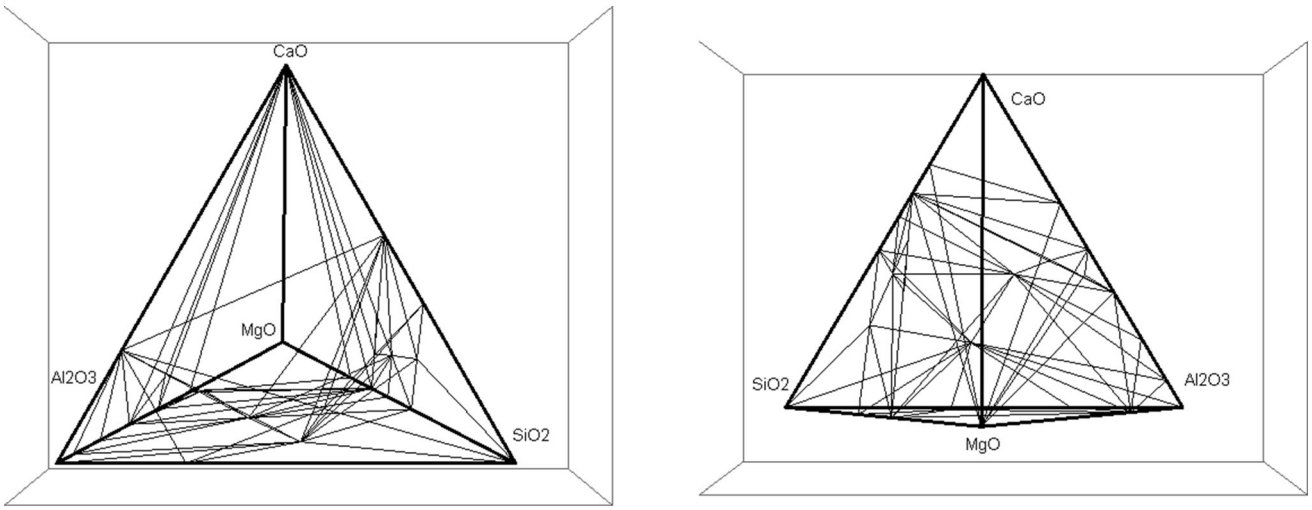

Fig. 3 The Al_2O_3-MgO-SiO_2-CaO quaternary system presented at different directions

$$\text{AKER} = \text{C2MS2} = \{22.05, 24.68, 33.56\},$$
$$\text{M4A5S2} = \{-24.63, 17.59, 0\},$$
$$\text{MONT} = \text{CMS} = \{19, 32.91, 29.39\}, \text{C3MS2} = \text{MERV} = \{18.35, 25.25, 41.69\},$$
$$\text{DIOP} = \text{CMS2} = \{27.7, 23.5, 21.05\},$$
$$\text{MA} = \{-35.83, 24.52, 0\},$$
$$\text{C3MA2} = \{-24.74, 20.25, 33.26\}$$

in which C = CaO, A = Al_2O_3 = corundum, M = MgO, S = SiO_2, AKER = akermenite, Diop = diopsite, MERV = mervinite.

With these coordinates of the binary and ternary components obtained using the originally derived transformations, the whole quaternary system in 3 dimensions including the known Alkemade lines are drawn using the commands given in Mathematica software (Fig. 2).

A novel program is then developed when an arbitrary composition X_A = wt.%Al_2O_3, X_B = wt.%MgO, X_C = wt.%SiO_2 and X_D = wt.% CaO is chosen for which it enables finding the Alkemade tetrahedron that contains the composition and calculates the distances to the apices of the tetrahedron. Thereafter applying the lever rule in the particular tetrahedron where X_A, X_B, X_C and X_D locate the wt.% or at. % of the existing minerals can be calculated after complete solidification of the melt is achieved (Fig. 3).

The 51 tetrahedra existing in the main Al_2O_3-MgO-SiO_2-CaO system were firstly defined in the program by inserting their apices coordinates as an input. Then, the program calculates the tetrahedron's volumes one by one using iterative determinant method and calculates the total volume of the quaternary system. When any composition is arbitrarily chosen ($X_A + X_B + X_C + X_D = 1$), the program directly transforms it into Cartesian coordinates xyz and then calculates the volumes of the 4 sub-tetrahedra formed when point XYZ divides each tetrahedron into 4; this is repeated by iteration for 51 tetrahedra forming the main tetrahedron. Another iteration sums the subtetrahedra volumes for each of the 51 tetrahedra and compares the results with their initial volumes determined earlier. The equality holds only when the right tetrahedron in which XYZ locates is reached and therefore summation of subtetrahedra volumes equalize the volume of its parent. As an example the two tetrahedra for which the apices are anorthite, forsterite, dyopside, enstatite and anorthite, cordierite, forsterite, spinel are given in Fig. 4. The third step of the program is to define the surfaces of the tetrahedron mathematically in which XYZ locates and then calculating the length of the segments initiating from the apices, crossing XYZ and joining the faces of the tetrahedron; the lever rule for quaternary system is then applied in order to find out the molecular fractions of the components forming the apices of the tetrahedron.

2.1 Validation of the Program by Comparing with the Experimental Results

The quaternary system A-M-S-C has already been studied experimentally by a few researchers[7,9,13–17] and its ternary components were already determined and published many years ago.[1,5,9–12] Based on the early experiments,[1] the proposed model is tested for two arbitrary ternary compositions, 1, 2, and two quaternary compositions, 3,4,5 and 6, given in Table 1.

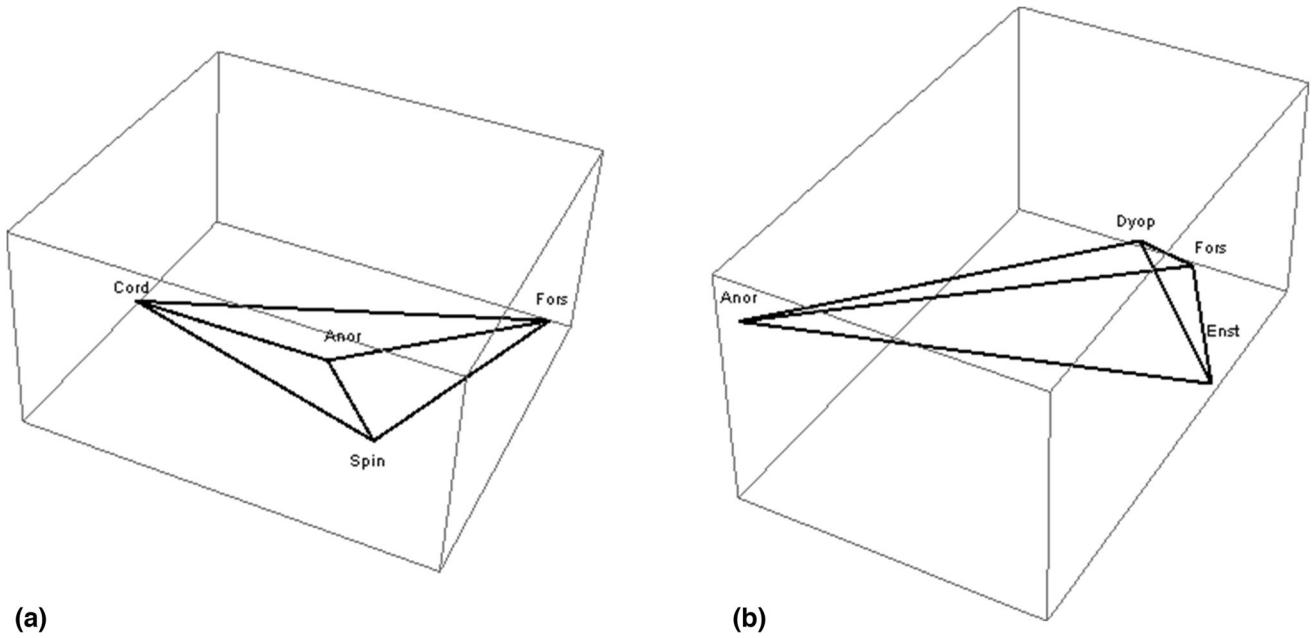

Fig. 4 The alkemade tetrahedra showing (a) Anorthite, cordierite, forsterite, spinel and (b) Anorthite, forsterite, dyopside, enstatite systems separately

The developed code is run for the experimental data (Table 1) given as input, the results are then compared with x-ray diffraction (XRD) findings and with the lever rule calculations performed on the Al_2O_3-MgO-SiO_2-CaO ternary system. Small numerical differences are possibly due to lever rule measurements for compositions 1 and 2.

Code outputs are provided as follows:

FOR THE LIQUID SLAG COMPOSITION 1:

Calculate which tetrahedron the liquid composition is in

The total sum of the main compounds must be "a + b + c + d = 100"

Enter % a associated with the first corner/compound Al2O3: 30

Enter % b associated with the second corner/compound MgO: 0

Enter % c associated with the third corner/compound SiO2: 40

Enter % d associated with the fourth corner/compound CaO: 30

The composition point 5 is in tetrahedron of number 2ans = "Tetrahedron #2: Gehlenite-Wollastonite-Akermanite-Anorthite"

The respective labels of the tetrahedron corners are:

Corner_1 = Gehlenite

Corner_2 = Wollastonite

Corner_3 = Akermanite

Corner_4 = Anorthite

Q1 being the intersection point of the line connecting the composition point 5 and the Corner_1 with the plane containing the respective corners 2,3 and 4, the distance between the composition point 5 and the point Q1 is:distance5Q1 = 4.6014distance1Q1 denoting the distance the between the Corner_1 and the intersection point Q1, the ratio distance5Q1/distance1Q1 is:ratio11 = 0.2265

Q2 being the intersection point of the line connecting the composition point 5 and the Corner_2 with the plane containing the respective corners 1,3 and 4, the distance between the composition point 5 and the point Q2 is:distance5Q2 = 5.9553distance2Q2 denoting the distance the between the Corner_2 and the intersection point Q2, the ratio distance5Q2/distance2Q2 is:ratio22 = 0.1854

Q3 being the intersection point of the line connecting the composition point 5 and the Corner_3 with the plane containing the respective corners 1,2 and 4, the distance between the composition point 5 and the point Q3 is:distance5Q3 = 0.0072distance3Q3 denoting the distance the between the Corner_3 and the intersection point Q3, the ratio distance5Q3/distance3Q3 is:ratio33 = 2.8498e−04

Q4 being the intersection point of the line connecting the composition point 5 and the Corner_4 with the plane containing the respective corners 1,2 and 3, the distance between the composition point 5 and the point Q4 is:distance5Q4 = 12.6114distance4Q4 denoting the distance the between the Corner_4 and the intersection point Q4, the ratio distance5Q4/distance4Q4 is:ratio44 = 0.5879

FOR THE LIQUID SLAG COMPOSITION 2:

Calculate which tetrahedron the liquid composition is in.

Table 1 Experimental slag compositions and equilibrium solid phases and corresponding code output

Liquid comp.#	wt.%Al_2O_3	wt.%MgO	wt.%SiO_2	wt.%CaO	Exp. output	Code output	Refs.
1	30	0	40	30	anorthite gehlenite wollastonite 0.1857	anorthite gehlenite wollastonite 0.1854^{+}	[1]
2	20	0	70	10	anorthite mullite cristobalite 0.4777	anorthite mullite cristobalite 0.4775^{++}	[1]
3	11.6	32	39.2	46	geh. aker undetermined quantitavely	geh.: 0.3931 aker: 0.2165	[12]
4	90	1	7	2	corundum, anorthite, mullite liquid t = 1352 °C above solidus	corundum 0.7697 anorthite 0.10 mullite 0.0950 spinel 0.0353	5(8)*
5	90	2.5	4	3.5	corundum spinel ca_6 liquid t = 1490 °C above solidus	corundum 0.6222 spinel 0.0883 ca6 0.1971 anorthite 0.0924	5(4)**
6	15	8	38.5	38.5	geh. aker. augite undetermined quantitavely	geh. 0.4053 aker 0.2653 (diopsite)^{x} 0.2202	[13]

* Batch #8 ** Batch #4 + wt.% wollastonite + + wt.% cristobalite x close to augite.

The total sum of the main compounds must be "a + b + c + d = 100"

Enter % a associated with the first corner/compound Al2O3: 20

Enter % b associated with the second corner/compound MgO: 0

Enter % c associated with the third corner/compound SiO2: 70

Enter % d associated with the fourth corner/compound CaO: 10

The composition point 5 is in tetrahedron of number 51ans = "Tetrahedron #51: Cord-Anorthite-Mullite-Cristobalite"

The respective labels of the tetrahedron corners are:

Corner_1 = Cord

Corner_2 = Anorthite

Corner_3 = Mullite

Corner_4 = Cristobalite

Q1 being the intersection point of the line connecting the composition point 5 and the Corner_1 with the plane containing the respective corners 2,3 and 4, the distance between the composition point 5 and the point Q1 is:distance5Q1 = 0.0031distance1Q1 denoting the distance the between the Corner_1 and the intersection point Q1, the ratio distance5Q1/distance1Q1 is:ratio11 = 1.4819e−04

Q2 being the intersection point of the line connecting the composition point 5 and the Corner_2 with the plane containing the respective corners 1,3 and 4, the distance between the composition point 5 and the point Q2 is:distance5Q2 = 23.4287distance2Q2 denoting the distance the between the Corner_2 and the intersection point Q2, the ratio distance5Q2/distance2Q2 is:ratio22 = 0.5000

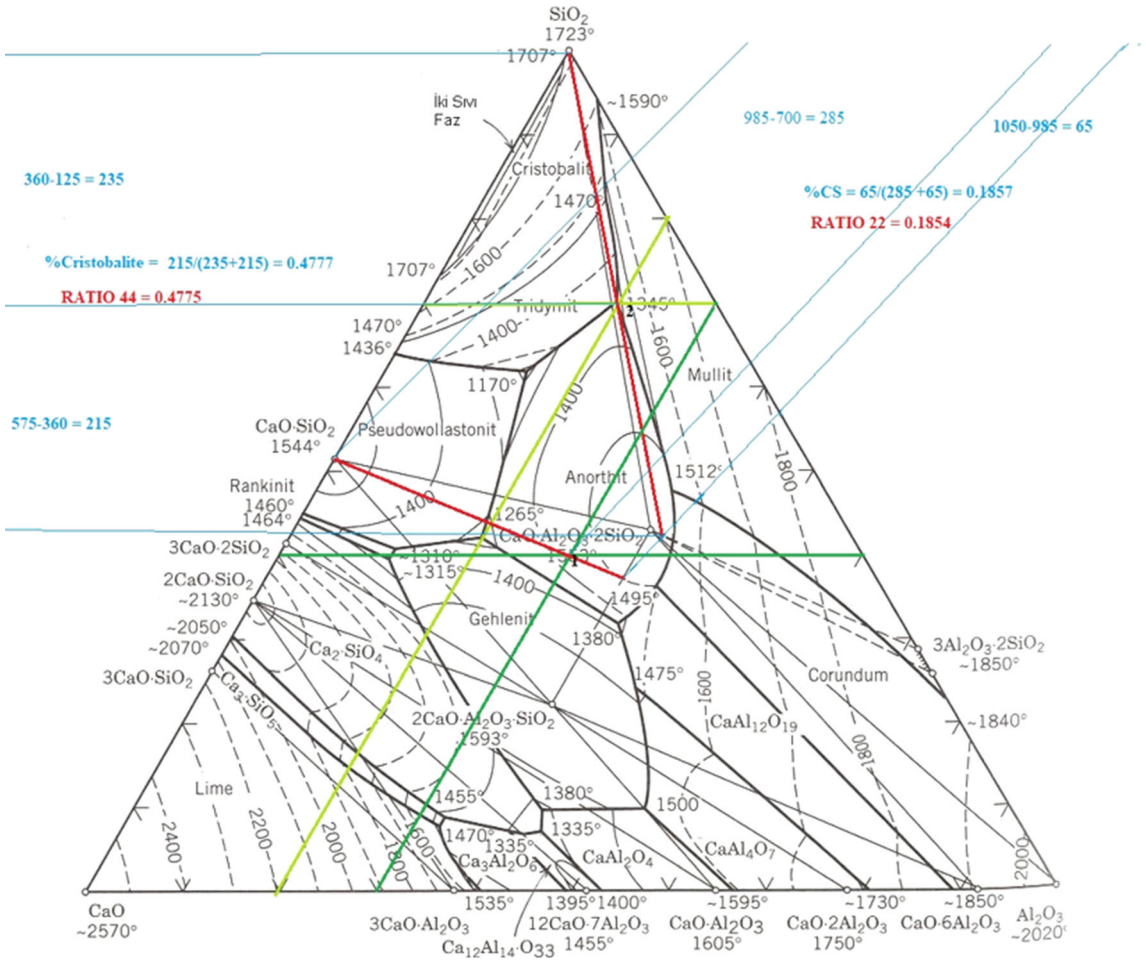

Fig. 5 Verification of the code for initial melt composition 1 and 2 as indicated on the Al_2O_3-SiO_2-CaO ternary equilibria

Q3 being the intersection point of the line connecting the composition point 5 and the Corner_3 with the plane containing the respective corners 1,2 and 4, the distance between the composition point 5 and the point Q3 is:distance5Q3 = 1.0912distance3Q3 denoting the distance the between the Corner_3 and the intersection point Q3, the ratio distance5Q3/distance3Q3 is:ratio33 = 0.0224

Q4 being the intersection point of the line connecting the composition point 5 and the Corner_4 with the plane containing the respective corners 1,2 and 3, the distance between the composition point 5 and the point Q4 is:distance5Q4 = 24.1745distance4Q4 denoting the distance the between the Corner_4 and the intersection point Q4, the ratio distance5Q4/distance4Q4 is:ratio44 = 0.4775

FOR THE LIQUID SLAG COMPOSITION 4:

It is calculated in which tetrahedron the composition point is located.

The total sum of the percent values of compounds must be "a + b + c + d = 100"

Enter % a associated with the first corner/compound Al2O3: 90

Enter % b associated with the second corner/compound MgO: 1

Enter % c associated with the third corner/compound SiO2: 7

Enter % d associated with the fourth corner/compound CaO: 2

The composition point 5 is in tetrahedron of number 19ans = "Tetrahedron #19: Anorthite-Corundum-Mullite-Spinel"

The respective labels of the tetrahedron corners are:

Corner_1 = Anorthite

Corner_2 = Corundum

Corner_3 = Mullite

Corner_4 = Spinel

Q1 being the intersection point of the line connecting the composition point 5 and the Corner_1 with the plane containing the respective corners 2,3 and 4, the distance between the composition point 5 and the point Q1 is:distance5Q1 = 5.2534distance1Q1 denoting the distance the between the Corner_1 and the intersection point Q1, the ratio distance5Q1/distance1Q1 is:ratio11 = 0.1000

Q2 being the intersection point of the line connecting the composition point 5 and the Corner_2 with the plane containing the respective corners 1,3 and 4, the distance between the composition point 5 and the point Q2 is:distance5Q2 = 29.3207distance2Q2 denoting the distance the between the Corner_2 and the intersection point Q2, the ratio distance5Q2/distance2Q2 is:ratio22 = 0.7697

Q3 being the intersection point of the line connecting the composition point 5 and the Corner_3 with the plane containing the respective corners 1,2 and 4, the distance between the composition point 5 and the point Q3 is:distance5Q3 = 2.0776distance3Q3 denoting the distance the between the Corner_3 and the intersection point Q3, the ratio distance5Q3/distance3Q3 is:ratio33 = 0.0950

Q4 being the intersection point of the line connecting the composition point 5 and the Corner_4 with the plane containing the respective corners 1,2 and 3, the distance between the composition point 5 and the point Q4 is:distance5Q4 = 0.8724distance4Q4 denoting the distance the between the Corner_4 and the intersection point Q4, the ratio distance5Q4/distance4Q4 is:ratio44 = 0.0353

The lever rule is then applied for composition 1 in order to calculate wt.% of wollastonite as indicated ratio 22 and for composition 2 to calculate wt.% of cristobalite as indicated ratio 44 given as above in output of the code. When the lever rule calculations based on geometrical measurements are observed in the Fig. 5, it is clearly seen that a nearly perfect match is obtained which necessarily validates the code.

For liquid slag compositions 3 and 6 provided in Ref. 14 and 15 based on EDS (Energy Dispersive Spectroscopy) and XRD analysis, the crystal configurations after solidification were determined to be mainly gehlenite, akermanite and gehlenite, akermanite and augite respectively which the latter is chemically close to diopsite. These results are also proved by the code. when it is run except the presence of wollastonite (CS) and C_3S_2 for composition 3 and CS for composition 4 appeared in the output. Composition 3 is determined to be located in tetrahedron #24 whereas composition 4 is calculated to be in tetrahedron#14. The missing components (CS, C_3S_2) which were not determined by XRD are most probably due to possible solid solutions for which the code does not work or to the imprecise measurements during XRD analysis for determining minor phases. For liquid slag composition 4 and 5 provided in Ref 5, a perfect match of solid phases including their relative amounts is also found (Table 1). The presence of liquid phase determined experimentally did not appear as an output due to limitation of the code which works for subsolidus case.

3 Conclusion

With this original algorithm developed using simple 3 D geometry and linear algebra principles, mathematical programming allows scientists to estimate the subsolidus phases in equilibrium including their relative amounts when an initial melt composition is entered into the system as an input. Before starting experimental studies and XRD/SEM characterizations, this algorithm will help reducing the costs and time consumption which is the main contribution of this research. Further studies can be done including non-stochiometric solid solutions such as $Mg_{1-x}(Al_2O_3)_{1+x}$ for which another loop repeating in a certain solid solution range ($a < x < b$ interval) can be devised in the code, also including liquid range for which non planar liquidus surfaces including their boundaries may be defined using line and surface integrals.

Acknowledgment We are grateful and respectful to the honor of Professor Mathematician Tahsin Çizenel deceised, author of Geometry books in 2D and 3D for his help in the derivation of transformations based on 3D Geometry.

References

1. E.M. Levin, C.R. Robbins, and H.F. McMurdie, *Phase Diagrams for Ceramists-1975 Supplement*. American Ceramic Society, Columbus, 1975.
2. J. Strigac, S. Sahu, and J. Majling, Phase Compatibility in the Systems $CaO-SiO_2-Fe_2O_3-SO_3$, $CaO-Al_2O_3-Fe_2O-SO_3$, and $SiO_2-Al_2O_3-Fe_2O_3-SO_3$, *Ceram. Silik.*, 1998, **42**, p 141–149.
3. K. Koch, G. Trömel, and G. Heinz, Das Hochofenschlackensystem Al_2O_3–CaO-MgO-SiO_2 bei 1600, 1500 und 1400 °C, *Arch. Eisenhüttenwes.*, 1975, **46**(3), p 165–171.
4. K. Koch, W. Fix, and G. Trömel, Die Phosphorgehalte im Eisen unter Schlacken des Systems $CaO-FeO_n-P_20_5-Si0_2$ bei 1600 °C, *Arch. Eisenhüttenwes.*, 1970, **41**(3), p 213–219.
5. B.A. Vaazquez, A. Caballero, and P. Pena, Quaternary System Al_2O_3-CaO-MgO-SiO_2: I, Study of the Crystallization Volume of Al_2O_3, *J. Am. Ceram. Soc.*, 2003, **86**(12), p 2195–2199.
6. B.A. Vaazquez, A. Caballero, and P. Pena, Quaternary System Al_2O_3-CaO-MgO-SiO_2: II Study of the Crystallization Volume of $MgAl_2O_4$, *J. Am. Ceram. Soc.*, 2005, **88**(7), p 1949–1957.
7. F.A. Hummel, *Introduction to Phase Equilibria in Ceramic Systems*. Routledge, UK, 2018. , **ISBN-10: 0367451832 ISBN-13: 978-0367451837**
8. K.G. Cox, J.D. Bell, and R.J. Pankhurst, *The Interpretation of Igneous Rock*. Springer, Berlin, 1993.
9. V.I. Lutsyk, A.E. Zelenaya, E.R. Nasrulin, 4D space models of quaternary systems for the phase diagrams graphics correction, in 3rd International Conference on Competitive Materials and Technology Processes (IC-CMTP3) IOP Publishing, IOP Conf. Series: Materials Science and Engineering, vol. 123 (2016), p. 012036.
10. E.F. Osborn, A. Muan, Phase equilibrium diagrams of oxide systems. System $CaO-Al_2O_3-SiO_2$, Plate 1 Figure 630; System $MgO-Al_2O_3-SiO_2$; Plate 3 Figure 712, in ed by C.R. Robbins, H.F. Mc Murdie Phase Diagrams for Ceramists (The American Ceramic Society, Colombus, Ohio, 1960).
11. A.H. De Aza, P. Pena, and S. De Aza, Ternary System Al_2O_3–MgO–CaO: I, Primary Phase Field of Crystallization of Spinel in

the Subsystem $MgAl_2O_4$-$CaAl_4O_7$-CaO-MgO, *J. Am. Ceram. Soc.*, 1999, **82**(8), p 2193–2203.
12. A.H. De Aza, J.E. Iglesias, P. Pena, and S. De Aza, 'Ternary System Al_2O_3-MgO-CaO: Part II, Phase Relationships in the Subsystem Al_2O_3-$MgAl_2O_4$-$CaAl_4O_7$, *J. Am. Ceram. Soc.*, 2000, **83**(4), p 919–927.
13. R.C. Devries, and E.F. Osborn, Phase Equilibria in High-Alumina Part of the System CaO-MgO-Al_2O_3-SiO_2, *J. Am. Ceram. Soc.*, 1957, **40**(1), p 6–15.
14. Z.E. Erkmen, E. Çataklı, and M. Lütfi Öveçoğlu, Characterisation and Crystallisation Kinetics of Glass Ceramics Developed from Erdemir Blast Furnace Slags Containing Cr_2O_3 and TiO_2 Nucleants, *Adv. Appl. Ceram.*, 2009, **108**(1), p 57–66.
15. F. Lai, M. Leng, J. Li, and Q. Liu, The Crystallization Behaviors of SiO_2-Al_2O_3-CaO-MgO-TiO_2 Glass-Ceramic Systems, *Curr. Comput. Aided Drug Des.*, 2020, **10**(794), p 1–13.
16. M. Kou, S. Wu, X. Ma et al., Phase Equilibrium Studies of CaO-SiO_2-MgO-Al_2O_3 System with Binary Basicity of 1.5 Related to Blast Furnace Slag, *Metall. Mater. Trans. B*, 2016, **47**(2), p 1093–1102.
17. D. Wang, M. Chen, Y. Jiang et al., Phase Equilibria Studies in the CaO-SiO_2-Al_2O_3-MgO System with CaO/SiO_2 Ratio of 0.9, *J. Am. Ceram. Soc.*, 2020, **103**(12), p 7299–7309.